Journal of New Materials for Electrochemical Systems 13, 315-320 (2010)

Preparation of Graphene/polypyrrole Composites for Electrochemical Capacitors

Yongqin Han, Bing Ding and Xiaogang Zhang

College of Material Science & Engineering, Nanjing University of Aeronautics and Astronautics, Nanjing 210016, China

Received: July 25, 2010, Accepted: October 20, 2010, Available online: November 15, 2010

Abstract: *Graphene/polypyrrole composites are synthesized by in situ polymerization under different mass ratios. The electrochemical performances of graphene, polypyrrole and composites have been investigated. The composites corresponding to the mass ratio 50:50 of graphene to pyrrole deliver an initial capacitance of 223 F/g at a current density of 0.5 A/g. The increased capacitance compared with pristine graphene and polypyrrole could be ascribed to the synergistic effect between graphene and polypyrrole. The cycling stability of the composites is also improved compared with that of polypyrrole. The loss of specific capacitance for the composite electrode is smaller and shows a stable cycle life, capacitance retention of the composites about 80% is found over 1200 cycles.*

Keywords: Graphene; Polypyrrole; Composites; Electrochemical capacitors

1. INTRODUCTION

Electrochemical capacitors, also known as supercapacitors, have attracted considerable attention in recent years for building up a green renewable energy environment. Depending on the nature of the charge-storage mechanism electrochemical capacitors are basically divided into two types, the electric double layer capacitor and the electrochemical pseudocapacitor[1-3]. The electrode materials used for the capacitors are normally carbon with a high surface area, noble metal oxides and conductive polymers [4-10]. Conductive polymers, such as polyaniline (PANI), polypyrrole (PPy), polythiophene and its derives, have attracted use for electrochemical capacitors because of a combination of high specific capacitance compared with carbon and a low cost compared with noble metal oxides. The frequent problems related to the application of conductive polymers are their poor chemical reversibility and short of cycling stability in aquoeus electrolytes. The combination of conductive polymers and extended inorganic species to form composite hybrid materials represents an opportunity for the design of materials with improved properties (stability, charge propagation dynamics) and enhanced specific capacitance.

Graphene, which consists of atom-thick sheets of carbon, organized in a honeycomb structure that resembles chicken wire, has received a rapidly growing research interest due to its long-range p-conjugation, yielding extraordinary thermal, mechanical, and electrical properties recently [11-14]. Compared with carbon nanotubes (CNTs), graphene is predicted as an excellent support material due to its high surface area, remarkable mechanical stiffness and excellent conductivity [15]. In addition, the production cost of graphene in large quantities is much lower than that of CNTs. Therefore graphene is a very promising candidate for new carbonaceous supports. The potential of using graphene-based materials for supercapacitor has attracted much attention very recently [16-18]. Specific capacitances of these materials are mainly limited by the agglomeration of graphene sheets and do not reflect the intrinsic capacitance of an individual graphene sheet [19].

Recently, different grahene/PANI composites have been prepared to be used as electrode materials for electrochemical capacitors [19-23]. The electrochemcial capacitance as well as the cycling stabilty of the composites have been improved compared with pristine graphene and PANI. Compared with PANI, PPy has drawn considerable attention due to its relatively better stability in ambient conditions and ease of synthesis. To the best of our knowledge, there are no reports related to graphene/PPy composites for electrochemical capacitor electrodes.

Here, for the first time grahene/PPy composites of different mass ratios have been synthesized by a very simple in situ polymerization method in aqueous media. The electrochemical performances of graphite oxide (GO), graphene, PPy, and graphene/PPy composite electrodes for supercapacitors have been investigated. The electrochemical tests demonstrate that the prepared composites posses enhanced specific capacitance and cycling stability.

*To whom correspondence should be addressed: Email: azhangxg@163.com
Phone/Fax:0086-25-52112626

2. EXPERIMENTAL

2.1. Materials

GO was synthesized from natural graphite (325mesh) that was kindly supplied by Shandong Pingdu Graphite Company (Qingdao, China). Pyrrole was purified by distillation under reduced pressure and stored in a refrigerator prior to use. Pyrrole and hydrazine hydrate were of analytical grade and purchased from Nanjing Chemcial Reagent Co. Ltd., (Nanjing, China). The oxidant ammonium persulfate (APS) was of analytical grade, and purchased from Shanghai Jiuyi Chemical Reagent Company (Shanghai, China). Acetylene black (200mesh) was purchased from Shanghai Heviant Enterprise Co. Ltd., (Shanghai, China). Polytetrafluoroethylene (PTFE) concentrate dispersion (FR301B, 60% in H_2O) was purchased from Shanghai 3F Co. Ltd ., (Shanghai, China). All other reagents were of analytical grade and used as supplied without further purification.

2.2. Preparation of GO

GO was prepared by the modified Hummers method [24]. Natural graphite powder was oxidized with $KMnO_4$ in concentrated H_2SO_4. 10g of graphite powder was added to 230 mL of cooled (0 °C) H_2SO_4 (98%). 30g of $KMnO_4$ and 5g $NaNO_3$ was added gradually with stirring and cooling to keep the temperature in the reactor at 0-4℃. The mixture was then stirred at 0-4℃ for 1d and stayed at room temperature for 4d. Then, 250mL of deinoized water was slowly added to the mixture. The reaction was terminated by adding 1L of deinoized water followed by 100 mL of 5% H_2O_2 solution. The solid product was separated by centrifugation, washed repeatedly with 5% HCl solution until sulphate could not be detected with $BaCl_2$, then washed 3–4 times with acetone and dried in a vacuum oven at 60°C for 24h.

2.3. Preparation of Graphene

Graphene was prepared by chemical conversion of GO according to the reported method [25]. In a typical experiment, 50mg of GO was dispersed in 50 mL of deionized water. Then 0.1mL (2M) of hydrazine hydrate was added, and the mixture was heated at 95°C for 2 h. Once the reaction was completed, the graphene was collected by filtration as a black powder. The obtained product was washed with deionized water several times to remove the excess hydrazine, and the final product was dried in a vacuum oven at 60°C for 24 h.

2.4. Preparation of PPy

70μL of pyrrole monomer (1 mmol) was added to 20 mL deionized water and stirred for 30min and then the oxidant APS (1mmol APS was added to 10mL deionized water) was added dropwise. The polymerization was allowed to proceed for 12h at 0-4 °C. The product obtained was filtered and washed with deionized water, and dried at 60°C for 24h under vacuum.

2.5. Preparation of Graphene/PPy composites

Graphene/PPy composites were prepared by *in situ* polymerization in aqueous media. The weight feed ratio of graphene to pyrrole was varied as 20:80, 50:50, and 80:20, and the resuting composites were named as GP20, GP50 and GP80, respectively. In a typical experiment, the obtained graphene was added into 50 mL deionized and sonicated for 30 min to obtain homogenous suspension. Pyrrole monomer was inserted to the above suspension under vigorous stirring. Then 10 mL APS (n_{APS}: $n_{Pyrrole}$=1 :1) aqueous solution was added dropwise. The polymerization was allowed to proceed for 12h at 0-4°C. The product obtained was filtered and washed with deionized water, and dried at 60°C for 24 h under vacuum.:

2.6. Characterization

Fourier-transform infrared spectroscopy (FTIR) spectra were recorded on a Bruker VECTOR22 FT-IR spectrometer by using pressed KBr pellets. Scaning electron microscope (SEM) mesurements were carried out by a HITACHI S-4800 scanning electron microscope. The specimens were platinum-coated prior to examination. X-ray diffraction (XRD) patterns were mesured on a Rigaku D/MAX-RC X-ray diffractometer with Cu K_α radiation.

All electrochemical experiments were carried out using a three-electrode system, in which platinum foils and saturated calomel electrode (SCE) were used as counter and reference electrodes, respectively. The working electrode was fabricated by mixing electroactive materials (GO, graphene, PPy and graphene/PPy composites), acetylene black and PTFE in a mass ration of 80:15:5 to make homogeneous mixture. The eletrodes were prepared at room temperature by pressing the homogeneous mixture on graphite current collector. The electrolyte was 1 M KCl. Cyclic voltammetry (CV), galvanostatic charge-discharge and electrochemical impedance spectroscopy (EIS) were performed with CHI750D electrochemical workstation. CV tests were done between -0.8 and 0.5 V at 10 mV/ s. Galvanostatic charge-discharge curves were measured at current density of 0.25, 0.5, 1 and 2 A/g. EIS measurements were carried out in the frequency range from 10^5 to 0.01Hz at open circuit potential with an ac perturbation of 5 mV. Galvanostatic cycling was performed between −0.8 and 0.5V at a constant current density of 0.5A/g for 1200 times using a LAND cell testing system (Szland CT2001C) to evaluate the cycling stability.

3. RESULTS AND DISCUSSION

3.1. Strucutre and morphology

In order to investigate the effect of the mass ratio of pyrrole to graphene on the electrochemical performances of graphene/PPy composites, three composites, GP20, GP50 and GP80, are prepared. Fig. 1 shows the FTIR spectra of GO, graphene,PPy, GP20,GP50 and GP80. Fig. 1a represents a typical IR spectrum of GO in accordance with the reported literature [26]. The C=O stretching of COOH groups situated at edges of GO sheets is observed at 1726 cm^{-1}. The absorptions due to the O–H bending vibration, epoxide groups and skeletal ring vibrations are observed around 1629 cm^{-1}. The absorption at 1386 cm^{-1} may be attributed to tertiary C–OH groups [27]. The IR spectrum of the graphene confirms reduction of GO sheets. Here the absorption due to the C=O group (1726 cm^{-1}) is absent and absorptions at 1629 and 1386 cm^{-1} are decreased very much in intensity. A new absorption band that appears near 1581cm^{-1} may be attributed to the skeletal vibration of the graphene sheets [28]. The GP20 and GP50 (Fig.1d) exhibit the characteristic absorption bands of pure PPy (Fig.1c), suggesting that PPy is successfully polymerized in the presence of graphene. Compared with the characteristic peaks of PPy, the peak at 1560 cm^{-1} (Fig.1 c) corresponding to the C=C backbone stretching of the PPy ring is downshifted to 1546cm^{-1} for GP20 (Fig.1d) and 1539 cm^{-1} for GP50 (Fig.1e) due to the π-π conjugate effect between

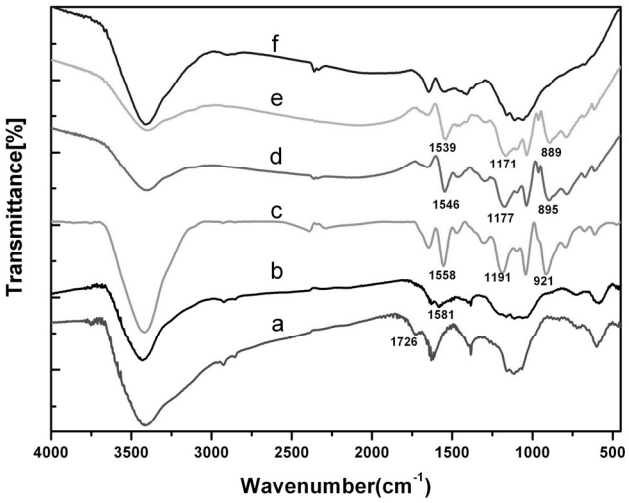

Figure 1. FTIR spectra of (a) GO;(b) graphene;(c)PPy ; (d) GP20;(e) GP50 and (f) GP80.

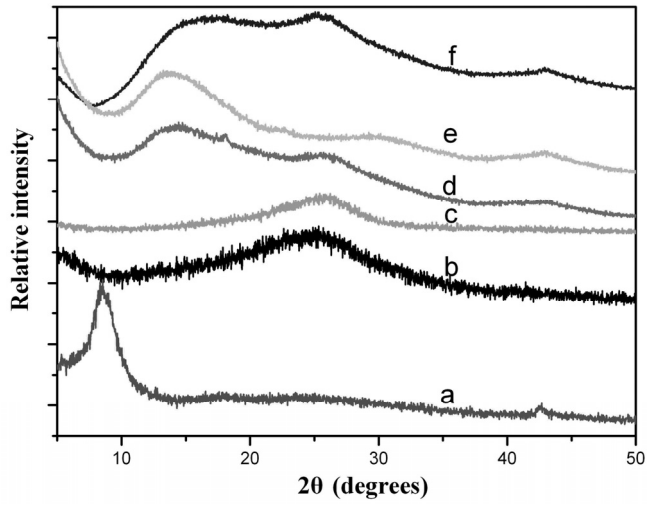

Figure 2. XRD patterns of (a) GO;(b) graphene;(c)PPy ; (d) GP20;(e) GP50 and (f) GP80.

graphene skeleton and PPy. The peak at 1191cm^{-1} is indicative of C-N stretching of PPy. For GP20 and GP50, this peak is also downshifted to 1177 cm^{-1} and 1171 cm^{-1} compared to pristine PPy, because of the hydrogen bonding between the remaining C-OH on graphene surface and nitrogen atoms in PPy. A small difference is noticed that the band centered at 919 cm^{-1} assigning to the bipolaron state of PPy [29] shifts to a lower wavenumber (895 and 889 cm^{-1}) for the composites. The shift might be attributed to the increased π-electron density induced by charge transfer [30]. The red shifts of the wavenumbers of the composites indicate that stronger interaction might exist between graphene and PPy in GP50 compared with GP20. For the case of GP80, only few PPy peaks with weak intensity are detected (Fig.1f), which is probably due to the lower content of PPy in the composites.

The XRD patterns of GO, graphene and the composites are

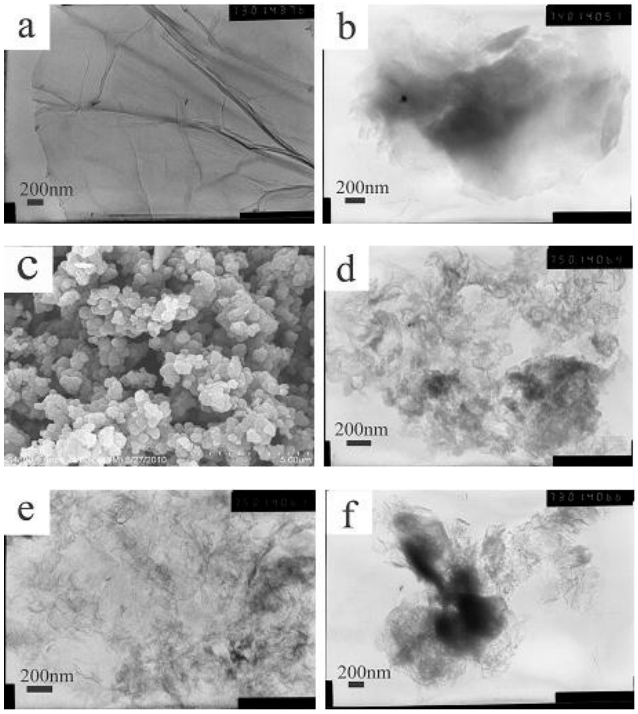

Figure 3. TEM and SEM images of (a) GO;(b) graphene;(c)PPy ;(d) GP20;(e) GP50 and (f) GP80.

shown in Fig. 2. From the XRD spectrum (Fig. 2a), a layer distance of 1.03 nm is calculated from the sharp peak at 2θ=8.4°for GO. This value can be attributed to the (001) reflection peak and might depend on the method of preparation and on the number of layers of water in the gallery space of GO [31]. One broad reflection peak centered at 2θ = 25.2° is observed in the XRD pattern of graphene (Fig. 2b), which can be correlated to an interlayer spacing of 0.35 nm in the graphene sample. The observed broad peak also indicates that the graphene sheets are loosely stacked, and it is different from the crystalline graphite. One broad peak at about 2θ = 25° in Fig.2c can be contributed to the amorphous structure of PPy. The GP20 and GP50 exhibit intense peaks at 2θ=18.1° (Fig.2d) and 2θ=13.7° (Fig.2e), respectively, probably corresponding to the crystalline order of PPy in the GP20 and GP50.

Fig. 3 shows TEM and SEM images for GO, graphene, PPy and the composites. The puckering feature of GO is observed in Fig. 3a, indicating that the exfoliation of the GO is improved by the sonication. As is shown in Fig.3b, after reduction the layered structure for graphene agglomerate can be observed. The agglomeration of the graphene layers can be attribute to the removal of the most functional groups from GO. The morphology of PPy prepared by in situ polymerization is submicron-spheres with diameter of 200-300 nm. From the image of SEM (Fig.3c), it can be found that these spheres are linked and packed together. Furthermore, the images reveal that the surfaces of PPy samples also possess rough and extended porous structures. This structure permits good access for the electrolyte molecules in PPy to form ionic conducting road. The composites morphology differs from that of pure graphene and PPy. It can be seen from Fig.3d - Fig. 3f that the dimension of the graphene

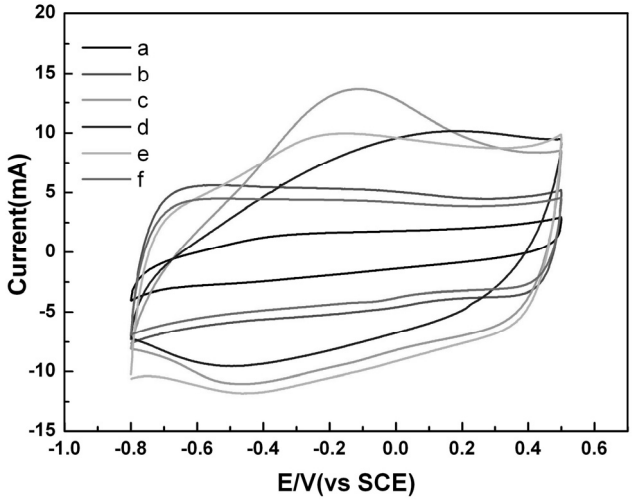

Figure 4. Cyclic voltammograms of (a) GO;(b) graphene;(c)PPy ; (d) GP20;(e) GP50 and (f) GP80 in 1M KCl at 10 mV/s.

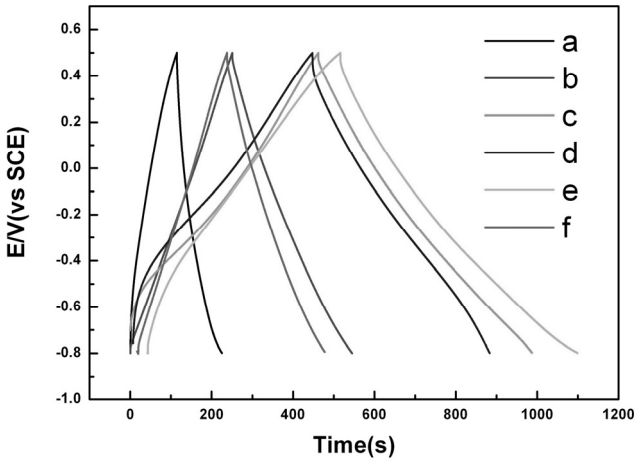

Figure 5. Galvastatic charge-discharge curve of (a) GO; (b) graphene; (c)PPy; (d) GP20; (e) GP50 and (f) GP80 at a constant current density of 0.5 A/g.

sheets decreases and the agglomeration of the graphene sheets is lowered in the composites, which might be due to the introduction of PPy. The short nano-fibrillar morphology of PPy in the composites might be induced by the residual C-OH on graphene sheets. It is worth noting that for GP20 PPys are liable to accumulate (Fig.3d) due to the high content of PPy. Similarly, graphene sheets are inclined to be agglomerated for GP80 due to the high content of graphene. GP80 provide homogeneous structure of both PPy and graphene sheets. The combination of graphene sheets and PPy might build an improved electron conducting network, thus enhancing the electrochemical performances of GP80.

3.2. Electrochemcial performances

Cyclic voltammetry (CV) and galvanostatic charge/discharge test are used to investigate the electrochemical capacitance performance of graphene/PPy composites. Fig. 4 shows the cyclic voltammograms of GO, graphene, PPy, GP20, GP50 and GP80 electrodes with scan rate of 10 mV/s in a potential range between -0.8 and 0.5V (*vs*. SCE). As can be seen, the CV curves of GO, graphene and the composites show roughly rectangular shape, indicating the capacitive behaviors [1]. From the peak current and CV curve enclosed area of the samples we can roughly estimate that graphene has a much larger capacitance as compared with GO. Similarly, among three composites, GP50 exhibit the best capacitance performance.

Charge/discharge curves of GO, graphene, PPy, GP20, GP50 and GP80 electrodes at a current density of 0.5A/g are shown in Fig. 5. The capacitance values are evaluated from charge–discharge cycling measurements, which are considered to be the most reliable. The specific capacitance values can be calculated from the equation:

$$C_m = \frac{C}{m} = \frac{I\Delta t}{\Delta v m} \quad (1)$$

Where I is the current of discharge, Δt is the discharge time, m is the mass of the active material, ΔV is the potential drop in the discharge progress, and C_m is the specific capacitance of the active material. The C_m values calculated from the charge/discharge curves are 43, 114, 201,167, 223 and 93 F/g for GO, grahene, PPy, GP20, GP50 and GP80, respectively. The specific capacitance of GP50 (223F/g) is much larger than that of each pristine component due to synergistic effect of composite formation. The enhanced specific capacitance may be attributed to the incorporation of PPy into graphene sheets and the interactions between graphene and PPy. Moreover, the C_m values of GP50 are 225, 223,189 and 160 F/g at current density of 0.25, 0.5, 1, and 2 A/g, respectively. These data show that the capacitance still retains about 71% of its original value when the current density increases as much as 8 times. The high capacitance retention of GP50 indicates a higher rate capability, which results from the synergistic effect of graphene and PPy.

EIS is further employed to monitor the electrochemical behavior of the electrodes. The Nyquist plots recorded for GO, graphene, PPy and GP50 are shown in Fig. 6. From the point intersecting with the real axis in the range of high frequency, the internal resistance (Rs) could be evaluated. The Rs of GO, graphene, PPy and GP50 are approximately 2.6Ω, 2.9Ω, 3.7Ω, 2.4Ω, respectively. In low frequency area, inclined lines are observed on impedances, the angles between the inclined lines and the real axes are between 45° and 90°, corresponding to the ion diffusion mechanism between Warburg diffusion and ideal capacitive ion diffusion. It can be seen from Fig.6 that compared with GO, the straight line part of graphene and PPy is more close to vertical line along the imaginary axis, suggesting they have better capacitive behaviors than GO. The angle between the inclined line and the real axe of GP50 composite electrode is similar to that of graphene and PPy, indicating that it also has good capacitive behavior.

The stability and reversibility of an electrode material are important for its use in an electrochemical capacitor. The cycle stabilities of PPy and GP50 are examined by means of cycle life test at a current density of 0.5A/g. It is found that the C_m of PPy electrode decreases 70% after 600 cycles due to its structural variety in cycle

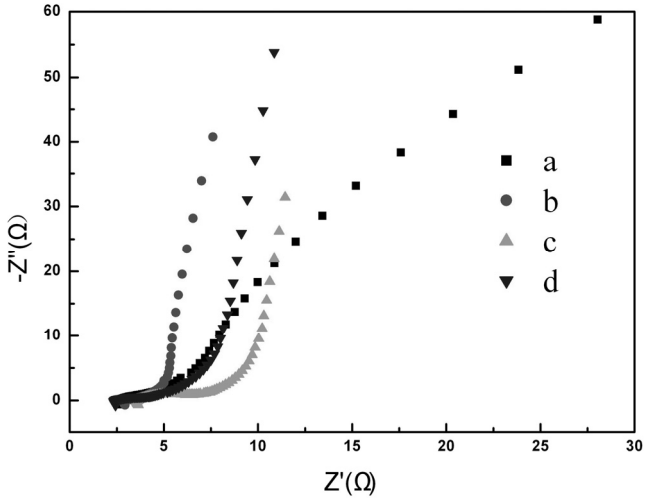

Figure 6. Nyquist plots of (a) GO;(b)graphene;(c)PPy and (d) GP50.

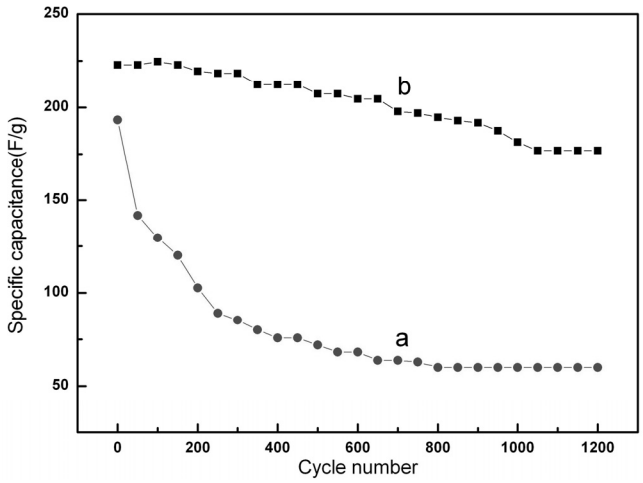

Figure 7. The specific capacitance change of (a) PPy and (b)GP50 at a constant current density of 0.5 A/g as a function of cycle number.

process, reflecting its poor cycling ability. Swelling and shrinkage of conducting polymers is well known and may lead to degradation of the electrode during cycling. However, GP50 have good cycling ability, retaining 80% after 1200 cycles. These results reveal that in GP50 the graphene sheets may preserve the PPy from mechanical changes (shrinkage and breaking) during long cycling, and enjoy high stability of the composite electrode for long cyclic life. So GP50 can be considered as promising materials in the application of electrochemical capacitors.

4. CONCLUSION

In summary, GO is reduced to graphene by hydrazine and graphene/PPy composites for electrochemical capacitor electrode are prepared by in situ polymerization. The performances for electrochemical capacitor electrodes of GO, graphene and the composites are investigated. Among the composites of different mass ratios, GP50 provide the best electrochemical performance. The incorporation of PPy in GP50 leads to the improved specific capacitance. The specific capacitance of GP50 is found to be 223 F/g at a constant current density of 0.5 A/g, which is higher than that of pristine graphene(114 F/g) and pure PPy (201 F/g). After 600 cycles of operation, the PPy electrode shows poor cycling stability, only maintaining 30% of its initial capacitance. The presence of graphene sheets in the composites can improve the cycling stability of GP50. The loss of specific capacitance for GP50 electrode is smaller and shows a stable cycle life, capacitance retention of about 80% is found over 1200 cycles. Our study suggests that GP50 have promising electrochemical performances for the applications as electrochemical capacitor electrodes.

5. ACKNOWLEDGEMENTS

This work was supported by National Basic Research Program of China (973Program) (No.2007CB209703), National Natural Science Foundation of China (No.20633040, No.20873064) and Postdoctoral Science Foundation of China (No. 20090461108).

REFERENCES

[1] B.E. Conway, J. Electrochem. Soc., 138, 1539 (1991).
[2] A. Burke, J. Power Sources, 91, 37 (2000).
[3] P. Simon, Y. Gogotsi, Nat. Mater., 7, 845 (2008).
[4] A.G. Pandolofo, A.F. Hollenkamp, J. Power Sources, 11, 157 (2008).
[5] C. Portet, J. Chmiola, Y. Gogotsi, S. Park, K.Lian, Electrochim. Acta, 53, 675 (2008).
[6] C.M. Yang, J. Am. Chem. Soc., 129, 20 (2007).
[7] V. D. Patake, S. M. Pawar, V. R. Shinde, T. P. Gujar, C.D. Lokhande, Curr. Appl. Phys., 10, 99 (2010).
[8] P. Ragupathy, D.H. Park, G. Campet, H.N. Vasan, S.J. Hwang, J.H. Choy, N. Munichandraiah, J. Phys. Chem. C, 113, 6303 (2009).
[9] S. Lee, M.S. Cho, J.D. Nam, Y. Lee, J. Nanosci. Nanotechnol., 8, 5036 (2008).
[10]J.F. Zang, S.J. Bao, C.M. Li, H.J. Bian, X.Q. Cui, Q.L. Bao, C.Q. Sun, J.Guo, K.R. Lian, J. Phys. Chem. C, 112, 14843 (2008).
[11]A.K. Geim, K.S. Novoselov, Nature Mater., 6, 183 (2007).
[12]J.C. Meyer, A.K. Geim, M.I. Katsnelson, K.S. Novoselov, T.J. Booth, S. Roth, Nature, 446, 60 (2007) .
[13]J.S. Bunch, A.M. van der Zande, S.S. Verbridge, I.W. Frank, D.M. Tanenbaum, J.M. Parpia, H.G. Craighead, P.L. McEuen, Science, 315, 490 (2007).
[14]X. Wang, L.J. Zhi, K. Müllen, Nano Lett., 8, 323 (2008).
[15]S. Stankovich, D.A. Dikin, G.H.B. Dommett, K.M. Kohlhaas, E.J. Zimney, E.A. Stach, R.D. Piner, S.T. Nguyen, R.S. Ruoff, Nature , 442, 282 (2006).
[16]M.D. Stoller, S. Park, Y. Zhu, J. An, R.S. Ruoff, Nano Lett. 8, 3498 (2008).
[17]Y. Wang, Z.Q. Shi, Y. Huang, Y.F. Ma, C.Y. Wang, M.M. Chen, Y.S. Chen J. Phys. Chem. C, 113, 13103 (2009).

[18]Y. Zhu, S. Murali, M.D. Stoller, A. Velamakanni, R.D. Piner, R.S. Ruoff, Carbon, 48, 2118 (2010).
[19]K. Zhang, L.L. Zhang, X.S. Zhao, J. Wu, Chem. Mater., 22, 1392 (2010).
[20]D.W. Wang, F. Li, J.P. Zhao, W.C. Ren, Z.G .Chen, J. Tan, Z.S. Wu, I. Gentle, G.Q. Lu, H.M. Chen, ACS Nano., 3, 1745 (2009).
[21]H.L. Wang, Q.L. Hao, X.J. Yang, L.D. Lu, X. Wang, Electrochem. Commun., 11, 1158 (2009).
[22]J .Yan, T. Wei, B. Shao, Z.J. Fan, W.Z. Qian, M.L. Zhang, F. Wei, Carbon, 48, 487 (2010).
[23]J. Yan, T. Wei, Z.J. Fan, W.Z. Qian, M.L. Zhang, F. Wei, J. Power Sources, 195, 3041 (2010).
[24]S.J. Park, R.S. Ruoff, Nat. Nanotech., 4, 217 (2010).
[25]S. Stankovich, D.A. Dikin, R.D. Piner, K.A. Kohlhaas, A. Kleinhammes, Y. Jia, Y. Wu, S.T. Nguyen, R.S. Ruoff, Carbon, 45, 1558 (2007).
[26]G.I. Titelman, V. Gelman, S. Bron, R.L. Khalfin, Y. Cohen, H. Bianco-Peled, Carbon, 43, 641 (2005).
[27]T. Szabo, O. Berkesi, P. Forgo, K. Josepovits, Y. Sanakis, D. Petridis, I. Dekany. Chem. Mater., 8, 2740 (2006).
[28]C. Nethravathi, M. Rajamathi, Carbon, 46, 11994 (2008).
[29]Y.C. Liu, Y.T. Lin, J. Phys. Chem. B, 107, 11370 (2003).
[30]W. Zhang, X. Wen, S. Yang, Langmuir ,19, 4420. (2003)
[31]N.I. Kovtyukhova, P.J. Ollivier, B.R. Martin, T.E. Mallouk, S.A Chizhik, E.V. Buzaneva, A.D. Gorchinskiy, Chem. Mater., 3, 771 (1999).